Investigating the Mechanical and Structural Properties of the Superior Sagittal Sinus

Darragh R. Walsh, Aisling M. Ross, David T. Newport, John J. E. Mulvihill

Abstract The meninges, which are a composite tissue surrounding the brain, play an important role in the mechanopathology of traumatic brain injury. Studies have demonstrated that the meninges are pivotal in mitigating the damaging strains placed on the cortex from both physiological and pathophysiological head movement, which can occur during dynamic events such as traffic accidents. Conversely, structures such as the falx and tentorium have been shown to induce large deleterious strains within the brain. Understanding the mechanical behaviour of these tissues is important to predict computational model brain strains. This study provides the first biomechanical and structural evaluation of the structures anatomically tethered to the falx cerebri, the superior sagittal sinus. We utilise uniaxial tensile testing, digital image correlation analysis and scanning electron microscopy on porcine superior sagittal sinus tissue to show that these structures are mechanically stiffer (with elastic moduli ranging from 33 to 58 MPa) than the properties that are typically assigned to them in computational models of traumatic brain injury (elastic modulus of 31.5 MPa). This work has the potential to improve the biofidelity of traumatic brain injury finite element models, thus improving crash reconstruction and injury prediction efforts.

Keywords Dura mater, finite element modelling, mechanical characterisation, TBI, venous sinuses.

I. INTRODUCTION

Traumatic brain injury (TBI) can be caused by rapid linear or rotational acceleration of the head experienced in vehicular collisions, explosions, falls, or assaults. The kinematics of TBI results in the application of damaging mechanical strains to cranial tissues, which may lead to acute and chronic brain function alteration [2]. An estimated 10 million people are affected annually by TBI [3]. The burden of mortality and morbidity that TBI imposes on society makes the condition a pressing public health and medical issue [4].

Improved vehicle design and the development of accident avoidance technologies have the potential to reduce the danger imposed by TBI in vehicle collisions [5]. Furthermore, the development of improved protective equipment has the potential to reduce the incidence of TBI sustained in participation in mainstream sports [6,7]. Finite element (FE) analysis is a tool which can provide fundamental insights into TBI injury mechanisms and therefore, can be utilised to improve the design of protective equipment and strategies to mitigate the prevalence of TBI [8].

The meningeal membrane is a critical composite tissue that protects the central nervous system (CNS). FE models have provided us with a plethora of evidence that the meninges have a significant influence on TBI mechanopathology [9]. In particular, fibrous extensions of the dura mater, the falx cerebri and tentorium cerebelli, have been identified as key structures in influencing TBI mechanopathology [9]. However, no studies currently exist detailing the mechanical response of the falx and tentorium, along with the intradural venous sinuses they are connected to. To date, the intradural sinuses have been largely ignored in the study of TBI mechanopathology. Experimental validation of computational modelling efforts have shown that accurately capturing the native tissue biomechanical properties in head models is essential for the accuracy of modelling results [10]. An improved knowledge of meningeal tissue properties is required if efforts are to improve preventative measures and advance vehicular design. In this study, we conduct mechanical and structural characterisation of the largest of the intradural venous sinuses, the superior sagittal sinus, which may aid in the biofidelity of head impact models.

D. R. Walsh is a PhD student in Biomechanics, D. T. Newport is a Senior Lecturer in the Department of Mechanical, Aeronautical and Biomedical Engineering and J. J. E. Mulvihill (john.mulvihill@ul.ie, +353 61-237719) is a Lecturer in the Department of Mechanical, Aeronautical and Biomedical Engineering at the University of Limerick. .

II. METHODS

Tissue Preparation

Pig tissue is frequently used in neuroscience applications due to the similarities between the cranial structures of pig and human [11,12] and due to the low availability of human donor tissue. Thus, 15 pig heads were sourced from a local abattoir for this study (Rosderra Meats, Nenagh, Ireland). 9 heads were designated for mechanical characterisation, while 3 heads were designated for structural analysis. Heads were dissected within 24 hours of animal euthanasia to prevent undesirable tissue degradation (see Figure 1 (A)) as per the methods described in our previous work. The intradural sinus tissue was then isolated from the surrounding dura mater tissue (see Figure 1 (B)). Isolation of the rectangular tissue sections was achieved using a pressing motion as described in [14] utilising a No. 22 blade scalpel (No. 22 Disposable Scalpel, Swann-Morton) while the sample rested on a dissection board. Note that both samples designated for both mechanical and structural characterisation were acquired in relation to the longitudinal axis of the superior sagittal sinus (see Figure 5 (A)).

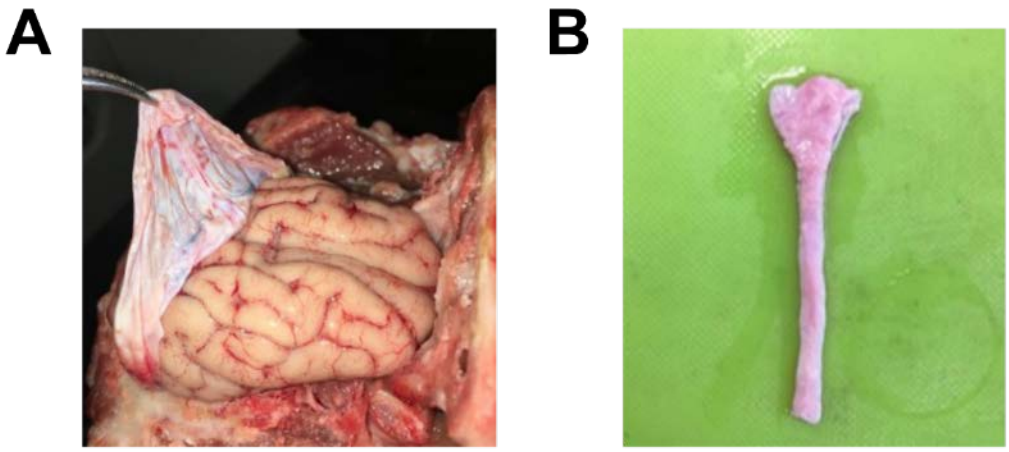

Fig. 1. (A) Dura mater tissue was removed from the porcine brain. (B) Superior sagittal sinus tissue is isolated from the native dura mater tissue. Note the total length of the porcine superior sagittal sinus is ~ 70 mm.

Test samples were then frozen in cryoprotectant agent [15] (to prevent mechanical and structural degradation) at -20^{o}C. Three distinct regions of the superior sagittal sinus were tested; the frontal, parietal and occipital region of the sinus. These regions were defined in relation to the lateral lobes of the brain they were subjacent to. Mechanical characterisation test specimens were cut into sections of ~ 30 x 4 mm (length x width) and then prepared by applying a speckle pattern to the sample surface for digital image correlation (DIC) analysis. The speckle application process, which was conducted utilising an ABEST airbrush (ABEST Dual action airbrush, ABESTOOLS) is as described below in Figure 2.

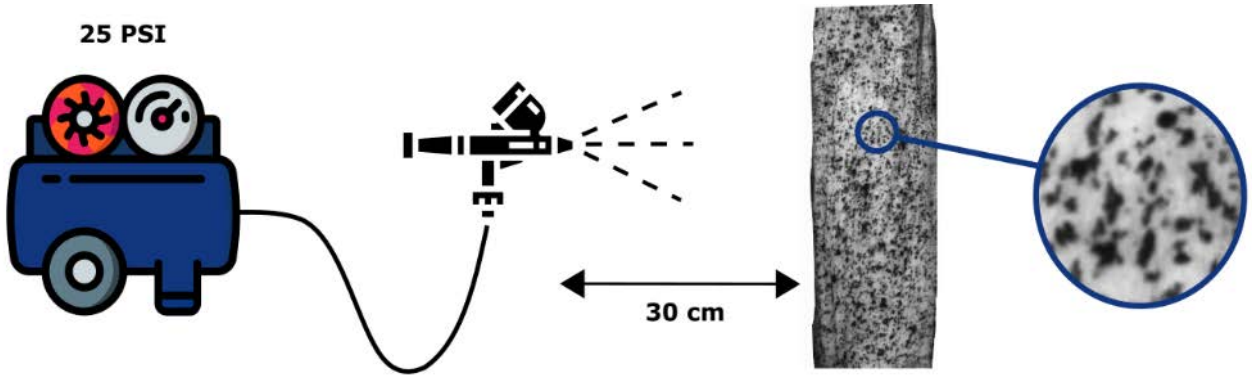

Fig. 2. Speckle pattern application for digital image correlation. Cancer Diagnostics Inc. (CDI) tissue staining dye, sprayed using an airbrush at a compressor pressure of 25 PSI with the airbrush nozzle 30 cm from the sample surface, was utilised. This produced speckles of ~ 40-60 µm diameter, which is desirable for high-resolution strain resolution.

Mechanical Characterisation

Prior to sample characterisation, sample geometrical measurements were acquired utilising noncontact photogrammetry methods similar to our previous work [16]. Images were acquired along the sample length and width. The sample geometry was then manually determined utilising the 'measure' function in ImageJ to determine sample cross-sectional area. Mechanical characterisation was then conducted utilising the Cellscale Biotester (CellScale, Canada). Samples were then secured in the testing clamps of the Biotester. The testing clamps were lined with gritted sandpaper and secured using a centrally positioned bolt with a torque of 50 cN.m, to mitigate sample slippage during characterisation. Samples were submerged in phosphate-buffered saline (PBS) solution at 37^{o}C throughout mechanical testing. Samples were preloaded to 0.1 N and then subjected to 10 preconditioning cycles to 1% strain (preconditioning serves to allow test samples to settle into the testing apparatus and to return the tissue to its in-situ stress configuration [17]). Samples were then stretched to a stretch of λ = 1.15 at a quasi-static strain rate of 1%/s for biomechanical characterisation.

Post-test DIC analysis utilising Cellscale's Labjoy software was conducted to determine local sample stretch throughout characterisation (see Figure 3 (C)). DIC stretch readings were determined utilising subset-based analysis [18] of the central region of test samples to avoid the well-documented effects of stress concentrations adjacent to sample grips [19,20]. The workflow for mechanical characterisation is as depicted in Figure 3.

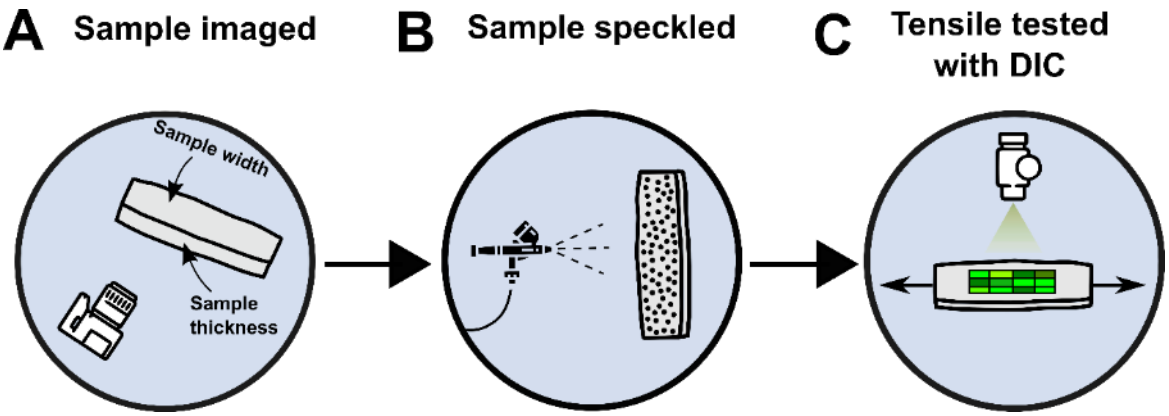

Fig. 3. Mechanical testing workflow. (A) Test samples are imaged to determine geometries utilising noncontact photogrammetry. (B) Samples are speckled prior to tensile testing. (C) Samples are tested in uniaxial tension and images are recorded throughout testing to allow for post-test DIC analysis.

As sample stretch was acquired from the sample's central region and samples had a uniform rectangular geometry, stretch readings were relatively homogenous, and therefore sample stretch was determined by averaging the DIC grid strains. In relation to sample stress calculation, Cauchy stress is typically used for hyperelastic, soft biological tissues [21]. In the case of an incompressible material, Cauchy stress is equal to Kirchoff stress [22]. As the dura mater is primarily composed of water like many other soft biological tissues [23], it is considered incompressible. Therefore, Cauchy stress for this study was determined by calculating the Kirchoff stress. Cauchy stress was thus calculated as:

$$\sigma_{Cauchy} = \lambda \sigma_{Engineering} \quad (1)$$

Where λ is sample stretch as determined from DIC analysis and engineering stress, $\sigma_{Engineering}$, is calculated as:

$$\sigma_{Engineering} = \frac{F}{A_0} \quad (2)$$

Where F is the measured force (determined from the load cells of the CellScale Biotester) and A_0 is the pre-test cross-sectional area, determined via pre-test noncontact photogrammetry.

To allow for quantitative comparison between the three test regions and to existing literature, elastic moduli were determined from the resulting Cauchy stress-strain curves. Moduli were calculated utilising a linear fit of the high strain, collagen-dominant region of the stress-stretch curves as described previously [16,24]. All linear fits had an R^2 value > 0.98 and were thus representative of the experimental data. As moduli were acquired from the high stiffness region of the stress-stretch curves, they are denoted as 'E_{stiff}' values.

Structural Characterisation

Biological tissue maceration involves chemical removal of all noncollagenic organic tissue components [25]. Superior sagittal sinus samples, separate to the mechanical characterisation samples, were macerated in 1 N NaOH solution for two weeks in order to remove all noncollagenic components such that the collagenic architecture of the tissue could be analysed. The alignment of the collagen fibres were quantitatively analysed utilising an ImageJ plugin, OrientationJ [26]. OrientationJ, an ImageJ plugin which calculates local orientation of fibres based on structure tensors [24], was utilised to study the preferential orientation of the collagen fibres in the porcine sagittal sinus.

Statistical Analysis

All statistical analyses were conducted utilising Prism software (GraphPad Prism 8.2.1). The normality of both the mechanical testing 'E_{stiff}' values were first assessed utilising a Shapiro-Wilk test. The normally distributed regional 'E_{stiff}' values were compared utilising an ordinary one-way analysis (ANOVA). A p-value of <0.05 was considered statistically significant.

III. RESULTS

The superior sagittal sinus, like many soft biological tissues, display a high degree of nonlinearity in its stress-strain behaviour [27] (as shown in the uniaxial stress-stretch curves shown in Figure 4 (A)). Table 1 summarises the regional elastic moduli values of the superior sagittal sinus. In Figure 4 (B), the elastic modulus result of [28], which is frequently assigned to the superior sagittal sinus in computational models [9], is shown for comparison to the results observed in the current study.

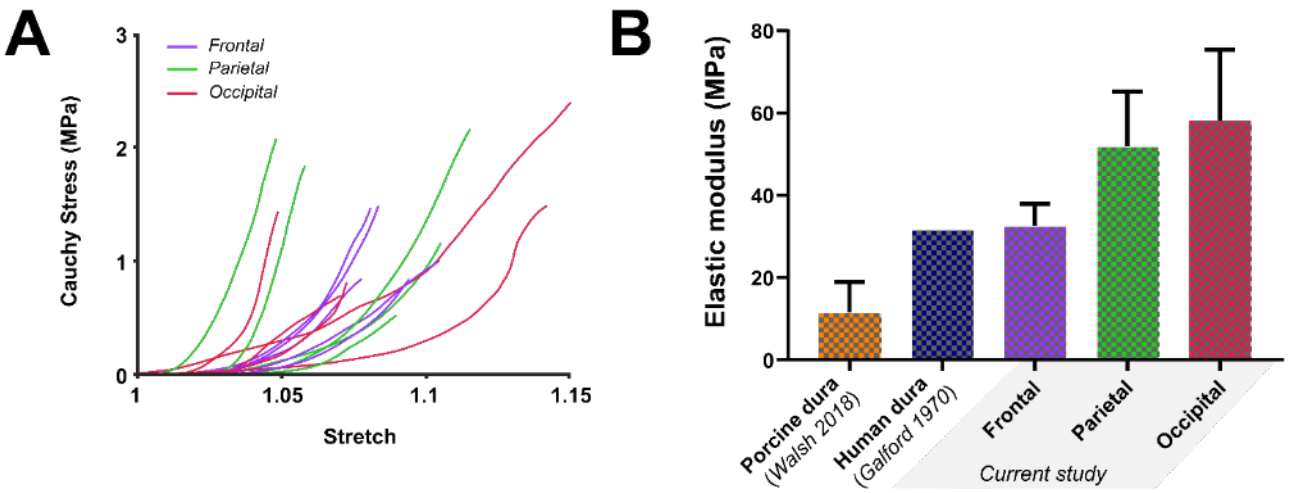

Fig. 4. (A) Plots of the Cauchy stress-stretch curves of the dural superior sagittal sinus samples tested in the vessel's longitudinal direction utilising uniaxial tensile testing. (B) Mean E_{stiff} results for the samples tested in the longitudinal test direction utilising uniaxial tensile testing. The value obtained by [26] of 31.5 MPa for native human dura mater tissue, is shown for reference. Also, the mean E_{stiff} value from our previous work [14] is included. Error bars represent standard error about the mean.

Figure 4 demonstrates that not only does the superior sagittal sinus tissue exhibit higher E_{stiff} values than porcine dura mater tissue, it also appears to trend toward a higher stiffness than the value assigned to sinuses on FE models based on the work of [28] on human dura mater. Evaluating the regional variation of the superior sagittal sinus, the tissue does trend toward a higher stiffness moving anterior to posterior. However, these regional differences did not prove to be statistically significant, possibly due to the high intra-sample variance commonly observed in meningeal tissues [23].

Table 1 summarises the elastic modulus results:

TABLE I
REGIONAL ELASTIC MODULI (VALUES REPRESENTED AS MEAN ± STANDARD ERROR)

Region	Elastic Modulus 'E_{stiff}' (MPa)
Frontal	32.6 ± 5.3
Parietal	51.9 ± 13.3
Occipital	58.1 ± 17.2

Structural Characterisation

The macerated bone surface layer of the dural sinus tissue is as shown in Figure 5 (A). As demonstrated in Figure 5 (B), the collagenic fibres of the bone surface layer of the dural sinus tissue appears to be preferentially aligned along the longitudinal direction of the sagittal sinus tissue.

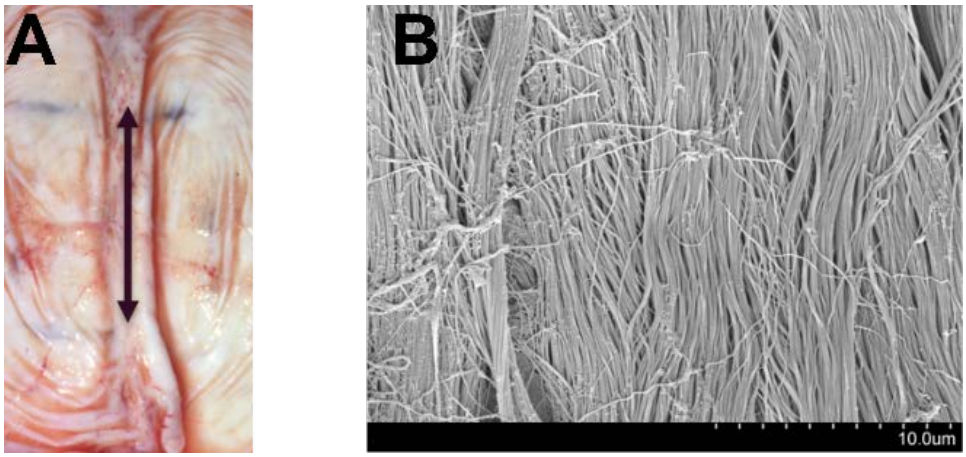

Fig. 5. (A) The longitudinal direction of the dural sinus is as depicted by the arrow. (B) Collagen fibres on the bone surface layer of macerated dural sinus tissue. Note that alignment of the image is as described in part (A) of current figure.

In line with the analysis of [29] on human dura mater collagenic architecture, the orientation distribution was analysed by generating histograms of the fibre orientations [29]. Similar analyses have been conducted previously on porcine skin tissue [30] and human ocular tissues [31]. The histogram is as shown in Figure 6 (B). Similar to the results of [29], the bone surface layer appears to exhibit moderate fibre alignment along the longitudinal direction of the sinus, as demonstrated by the uneven distribution of fibre orientation in the histogram. This may explain the tissue's significant mechanical stiffness, as collagenic alignment is a major factor in soft tissue biomechanics [32].

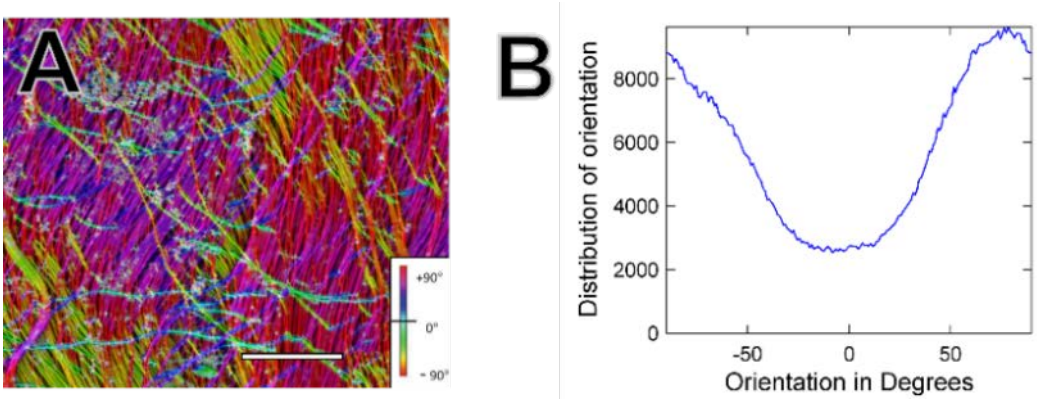

Fig. 6. (A) Representative colour map analysis of the SEM image shown in Figure 5. The colour of each fibre corresponds to the preferential local orientation of each fibre (in degrees, where 0^o is as indicated by the black line of the legend). This analysis was conducted through structure tensor analysis utilising OrientationJ software. (B) Histogram of the fibre orientation of (A).

IV. Discussion

FE modelling of head impacts is used extensively in the automobile industry for the optimisation of vehicle design [5]. A major metric for assessing the severity of a concussive impact in FE modelling is the evaluation of brain strains [33]. The cranial meninges are a group of tissues which encase and support homeostasis of the brain [34]. Previous FE modelling analyses have demonstrated that both the dura mater [35,36] and the pia-arachnoid mater [37] appear to provide protection to the cortex during TBI insults. However, in contrast to the potentially shielding role of the dura mater and pia-arachnoid complex, the falx cerebri potentially negatively influences the force propagation of deleterious effects of TBI on the brain. Numerous studies have demonstrated that the falx has the potential to induce significant localised TBI brain strains [9,38,39]. The large stiffness gradient between the brain, which is one of the softest tissues in the body [40], and the adjacent dural structures has been shown to cause large deformations within deep brain structures [9]. The work of [38] was the first to investigate the phenomenon of falx-induced brain strains utilising three-dimensional FE head models. Biofidelic FE head models, based on patient-specific anatomical data, with and without the falx and tentorium structures. To assess the propensity of the falx and tentorium to influence TBI brain strains, the authors simulated a reconstructed concussive sport accident on these models. They identified that the addition of the falx and tentorium to the head models resulted in a decrease in brain tissue strains in peripheral brain regions with an increase in strain within deep brain structures, such as the corpus callosum. The authors hypothesise that the mechanism of this localised strain observed within the corpus callosum is related to the stiff falx consolidating movement of the cerebral hemispheres. The authors conclude that the steep stiffness gradient between the falx and the brain tissue which they likely contact during TBI results in the deleterious localised strain heterogeneity.

A recent study on the etiology of falx and tentorium-induced brain trauma is the work of [9]. Similar to the work of [38], the authors utilised three-dimensional FE head models with and without the falx cerebri [38]. Interestingly, the authors also evaluated the impact of altering the material properties (elastic modulus) assigned to the falx. In simulating the impact conditions which resulted in the loss of consciousness of an American Football athlete, the authors found that a control model, with falx stiffness equal to that of native dura mater tissue (31.5 MPa), the corpus callosum strain was 35%. Further simulations exploring the role of the falx identified that softening and stiffening the model's falx resulted in a decrease (32% strain) and an increase (41% strain) in model corpus callosum strain, respectively. Furthermore, the authors found that completely removing the falx from the model resulted in a 50% reduction in corpus callosum strain to 17% strain. To explain the clearly influential role of the falx, the authors provide a novel hypothesis for the corpus callosum strains. They suggest that deformation of the distal, free edge of the falx following dynamic impacts may result in the falx contacting the cerebral hemispheres superior to the corpus callosum. The stiffness gradient between the falx and corpus callosum may then account for the strain concentrations observed in the inferior corpus callosum. This study highlights the critical importance of biofidelically modelling the meningeal tissues for brain injury prediction and prevention

purposes.

As a result of the anatomical connection between the superior sagittal sinus and the falx, it is likely the sinus has the propensity to influence falx biomechanical behaviour in finite element models. To date, many studies have evaluated the mechanical behaviour of native dura mater tissues in porcine [16,35] and human tissues [23,42,43]. However, there is a paucity of studies investigating the properties of the intradural sinuses. Our previous work [13], also on porcine tissue, was the first to explore the mechanics of the largest of the intradural sinuses, the superior sagittal sinus. Our findings identified, for the first time, potential stiffness differences between the native dura mater and the superior sagittal sinus. However, our previous work did not incorporate digital image correlation analysis, which is important for accurate strain assessment [20], did not evaluate regional variations within the superior sagittal sinus, and did not evaluate the structural alignment of the tissue. As a result of the dearth of constitutive data on the sinuses, computational models which include the structures represent them with the same mechanical properties as the native dura mater tissue (elastic modulus of 31.5 MPa) [28]. Here we show that the superior sagittal sinus, at least in porcine tissue, is stiffer (with elastic moduli ranging from 33 – 58 MPa) than the value typically assigned in human finite element models (as depicted in Figure 4 (B)). In addition, when comparing the stiffness results to dura mater tissue of the same species (Figure 4 (B)), the porcine superior sagittal sinus appears to exhibit larger stiffness than the native porcine dura. A limitation of this comparison is that our previous work did not incorporate DIC analysis [13]. However, even with this considered, the sinus tissue does appear to be notably stiffer than the native dura. These findings warrant further investigation in human tissues. We hypothesise that if these findings translate to human tissues, it may influence the FE modelling of TBI-induced load propagation to the cortex by influencing the modelled response of the superior sagittal sinus-falx interface.

Scanning electron microscopy analysis combined with tissue maceration techniques were utilised to study local fibre alignment in an attempt to explain the tissue's large mechanical stiffness. The alignment of collagen fibres, the main structural protein in soft biological tissues [44], is a major factor in a tissue's mechanical behaviour. Through the use of an orientation analysis tool in ImageJ [26], we show that the superior sagittal sinus demonstrates preferential alignment along its longitudinal axis (as depicted in Figure 6), which may explain its large stiffness.

Wall thickness is another important factor for the FE modelling of vascalature [45]. A recent microscopic anatomy investigation on the variability of dural sinus wall thickness provided a comprehensive overview of regional human sinus wall geometrical properties by [46]. The evolution of MRI-based anatomical modelling can also facilitate the development of patient-specific human head models with a high degree of geometrical accuracy. Thus, regional analysis of the venous sinus wall thickness was not a focus of this investigation.

A limitation of the structural analysis performed in this study is that it only evaluates the surface layer of the dural sinus tissue. Thus, future work will focus on the use of three-dimensional structural analysis techniques, such as second harmonic generation microscopy [47]. Future work will also investigate the mechanical behaviour of the dural sinuses in human tissue for improved translatability of results. It should also be noted that the quasi-static strain rate utilised in this study may not represent the behaviour of this tissue at more dynamic, TBI-relevant strain rates. It is currently unclear if the native dura mater tissue has strain rate dependency as it has not been investigated in the literature. However, despite these limitations, the results suggest that dural sinuses are stiffer than native dura mater tissue and these results warrant further investigation for improving the biofidelity of TBI FE models.

V. CONCLUSIONS

This work represents the first mechanical and structural characterisation of the superior sagittal sinus, the largest of the intradural venous sinuses. The sinus appears to have higher mechanical stiffness than the value that is currently assigned to the tissues in finite element models of TBI. Structural analysis utilising scanning electron microscopy suggests that this may be due to the collagenic fibre alignment of the sinus tissue. These results may aid in improving the biofidelity of head impact simulations for accident reconstructions.

VI. REFERENCES

[1] Rezakhaniha, R., Agianniotis, A., et al. Experimental investigation of collagen waviness and orientation in the arterial adventitia using confocal laser scanning microscopy. *Biomech. Model. Mechanobiology*, 2012. 11(3): p. 461-473

[2] Gavett, B.E., Stern, R.A., and McKee, A.C. Chronic traumatic encephalopathy: a potential late effect of sport-related concussive and subconcussive head trauma. *Clinics in sports medicine*, 2011. 30(1): p. 179-88, xi

[3] Zaloshnja, E., Miller, T., Langlois, J.A., and Selassie, A.W. Prevalence of long-term disability from traumatic brain injury in the civilian population of the United States, 2005. *J Head Trauma Rehabil*, 2008. 23(6): p. 394-400

[4] Hyder, A.A., Wunderlich, C.A., Puvanachandra, P., Gururaj, G., and Kobusingye, O.C. The impact of traumatic brain injuries: a global perspective. *NeuroRehabilitation*, 2007. 22(5): p. 341-53

[5] Crandall, J.R., Bhalla, K.S., and Madeley, N.J. Designing road vehicles for pedestrian protection. *BMJ (Clinical research ed.)*, 2002. 324(7346): p. 1145-1148

[6] Viano, D.C., Pellman, E.J., Withnall, C., and Shewchenko, N. Concussion in professional football: performance of newer helmets in reconstructed game impacts--Part 13. *Neurosurgery*, 2006. 59(3): p. 591-606; discussion 591-606

[7] Harmon, K.G., Drezner, J.A., et al. American Medical Society for Sports Medicine position statement: concussion in sport. *British Journal of Sports Medicine*, 2013. 47(1): p. 15

[8] Gu, L., Chafi, M.S., Ganpule, S., and Chandra, N. The influence of heterogeneous meninges on the brain mechanics under primary blast loading. *Composites Part B: Engineering*, 2012. 43(8): p. 3160-3166

[9] Hernandez, F., Giordano, C., et al. Lateral impacts correlate with falx cerebri displacement and corpus callosum trauma in sports-related concussions. *Biomech. Model. Mechanobiology*, 2019. 18(3): p. 631-649

[10] Ganpule, S., Alai, A., Plougonven, E., and Chandra, N. Mechanics of blast loading on the head models in the study of traumatic brain injury using experimental and computational approaches. *Biomech. Model. Mechanobiology*, 2013. 12(3): p. 511-531

[11] MacManus, D.B., Pierrat, B., Murphy, J.G., and Gilchrist, M.D. Region and species dependent mechanical properties of adolescent and young adult brain tissue. *Scientific Reports*, 2017. 7(1): p. 13729

[12] Sauleau, P., Lapouble, E., Val-Laillet, D., and Malbert, C.H. The pig model in brain imaging and neurosurgery. *Animal : an international journal of animal bioscience*, 2009. 3(8): p. 1138-51

[13] Walsh, D.R., Ross, A.M., et al. Regional mechanical and biochemical properties of the porcine cortical meninges. *Acta Biomaterialia*, 2018. 80: p. 237-246

[14] Fossum, T.W., "Small Animal Surgery Textbook - E-Book". 2013: Elsevier Health Sciences.

[15] Müller-Schweinitzer, E. Cryopreservation of vascular tissues. *Organogenesis*, 2009. 5(20046671): p. 97-104

[16] Walsh, D.R., Ross, A.M., et al. Regional mechanical and biochemical properties of the porcine cortical meninges. *Acta Biomater*, 2018

[17] Walsh, M.T., Cunnane, E.M., et al. Uniaxial tensile testing approaches for characterisation of atherosclerotic plaques. *Journal of Biomechanics*, 2014. 47(4): p. 793-804

[18] Jones, E.M.C. and Iadicola, M.A. A Good Practices Guide for Digital Image Correlation. 2018.

[19] Anssari-Benam, A., Legerlotz, K., Bader, D.L., and Screen, H.R.C. On the specimen length dependency of tensile mechanical properties in soft tissues: Gripping effects and the characteristic decay length. *Journal of Biomechanics*, 2012. 45(14): p. 2481-2482

[20] Cooney, G.M., Lake, S.P., et al. Uniaxial and biaxial tensile stress-stretch response of human linea alba. *J. Mech. Behav. Biomed. Mater.*, 2016. 63: p. 134-140

[21] Holzapfel, G.A., Mulvihill, J.J., Cunnane, E.M., and Walsh, M.T. Computational approaches for analyzing the mechanics of atherosclerotic plaques: A review. *Journal of Biomechanics*, 2014. 47(4): p. 859-869

[22] Khanafer, K., Schlicht, M.S., and Berguer, R. How Should We Measure and Report Elasticity in Aortic Tissue? *European Journal of Vascular and Endovascular Surgery*, 2013. 45(4): p. 332-339

[23] De Kegel, D., Vastmans, J., et al. Biomechanical characterization of human dura mater. *Journal of the Mechanical Behavior of Biomedical Materials*, 2018. 79: p. 122-134

[24] Monea, A.G., Baeck, K., et al. The biomechanical behaviour of the bridging vein–superior sagittal sinus complex with implications for the mechanopathology of acute subdural haematoma. *J. Mech. Behav. Biomed. Mater.*, 2014. 32: p. 155-165

[25] Sangiorgi, S., Manelli, A., Protasoni, M., Ronga, M., and Raspanti, M. The collagenic structure of human digital skin seen by scanning electron microscopy after Ohtani maceration technique. *Annals of Anatomy-Anatomischer Anzeiger*, 2005. 187(1): p. 13-22
[26] Rezakhaniha, R., Agianniotis, A., et al. Experimental investigation of collagen waviness and orientation in the arterial adventitia using confocal laser scanning microscopy. *Biomech Model Mechanobiol*, 2012. 11(3-4): p. 461-73
[27] Maikos, J.T., Elias, R.A.I., and Shreiber, D.I. Mechanical properties of dura mater from the rat brain and spinal cord. *Journal of Neurotrauma*, 2008. 25(1): p. 38-51
[28] Galford, J.E. and McElhaney, J.H. A viscoelastic study of scalp, brain, and dura. *Journal of Biomechanics*, 1970. 3(2): p. 211-221
[29] Protasoni, M., Sangiorgi, S., et al. The collagenic architecture of human dura mater. *J Neurosurg*, 2011. 114(6): p. 1723-30
[30] Jor, J.W.Y., Nielsen, P.M.F., Nash, M.P., and Hunter, P.J. Modelling collagen fibre orientation in porcine skin based upon confocal laser scanning microscopy. *Skin Research and Technology*, 2020. 17(2): p. 149-159
[31] Ávila, F.J. and Bueno, J.M. Analysis and quantification of collagen organization with the structure tensor in second harmonic microscopy images of ocular tissues. *Appl. Opt.*, 2015. 54(33): p. 9848-9854
[32] Jason, T.M., Ragi, A.I.E., and David, I.S. Mechanical Properties of Dura Mater from the Rat Brain and Spinal Cord. *Journal of Neurotrauma*, 2008. 25(1): p. 38-51
[33] Li, J., Zhang, J., Yoganandan, N., Pintar, F., and Gennarelli, T. Regional brain strains and role of falx in lateral impact-induced head rotational acceleration. *Biomedical sciences instrumentation*, 2007. 43: p. 24-29
[34] Rua, R. and McGavern, D.B. Advances in Meningeal Immunity. *Trends in molecular medicine*, 2018. 24(6): p. 542-559
[35] MacManus, D.B., Pierrat, B., Murphy, J.G., and Gilchrist, M.D. Protection of cortex by overlying meninges tissue during dynamic indentation of the adolescent brain. *Acta Biomaterialia*, 2017. 57: p. 384-394
[36] Gu, L., Chafi, M.S., Ganpule, S., and Chandra, N. The influence of heterogeneous meninges on the brain mechanics under primary blast loading. *Composites: Part B, Engineering*, 2012. 43(8): p. 3160-3166
[37] Scott, G.G., Margulies, S.S., and Coats, B. Utilizing multiple scale models to improve predictions of extra-axial hemorrhage in the immature piglet. *Biomech. Model. Mechanobiology*, 2016. 15(5): p. 1101-1119
[38] Ho, J., Zhou, Z., Li, X., and Kleiven, S. The peculiar properties of the falx and tentorium in brain injury biomechanics. *Journal of Biomechanics*, 2017. 60: p. 243-247
[39] Li, J., Zhang, J., Yoganandan, N., Pintar, F., and Gennarelli, T. Regional brain strains and role of falx in lateral impact-induced head rotational acceleration. *Biomedical sciences instrumentation*, 2007. 43: p. 24-9
[40] Budday, S., Ovaert, T.C., Holzapfel, G.A., Steinmann, P., and Kuhl, E. Fifty Shades of Brain: A Review on the Mechanical Testing and Modeling of Brain Tissue. *Archives of Computational Methods in Engineering*, 2019
[41] Halldin, P., Aare, M., Kleiven, S., and von Holst, H. Improved helmet design and test methods to reduce rotational induced brain injuries. *Proceedings of RTO Specialist Meeting, the NATO's Research and Technology Organization (RTO)*.
[42] van Noort, R., Black, M.M., Martin, T.R.P., and Meanley, S. A study of the uniaxial mechanical properties of human dura mater preserved in glycerol. *Biomaterials*, 1981. 2(1): p. 41-45
[43] Wolfinbarger Jr, L., Zhang, Y., et al. Biomechanical aspects on rehydrated freeze-dried human allograft dura mater tissues. *J Appl Biomater*, 1994. 5(3): p. 265-270
[44] Gaul, R.T., Nolan, D.R., and Lally, C. Collagen fibre characterisation in arterial tissue under load using SALS. *J. Mech. Behav. Biomed. Mater.*, 2017. 75: p. 359-368
[45] Shang, E.K., Nathan, D.P., et al. Local wall thickness in finite element models improves prediction of abdominal aortic aneurysm growth. *Journal of Vascular Surgery*, 2015. 61(1): p. 217-223
[46] Balik, V., Uberall, I., et al. Variability in Wall Thickness and Related Structures of Major Dural Sinuses in Posterior Cranial Fossa: A Microscopic Anatomical Study and Clinical Implications. *Operative neurosurgery (Hagerstown, Md.)*, 2019. 17: p. 88-96
[47] Chen, X., Nadiarynkh, O., Plotnikov, S., and Campagnola, P.J. Second harmonic generation microscopy for quantitative analysis of collagen fibrillar structure. *Nature protocols*, 2012. 7: p. 654-69